Comparing Dynamic Model and Flight Control of Plus and Cross Quadcopter Configurations

Khalid Mohsin Ali
Department of Computer EngineeringTechnology, Faculty of InformationTechnology, Imam Ja'afar Alsadiq University
Iraq

Alaa Abdulhady Jaber
Assistant Professor
Mechanical Engineering Department
University of Technology
Iraq

This research investigates and demonstrates the fundamental differences in performance and operation of both the cross and quadcopter configurations. The system's nonlinear dynamic model was first derived and implemented in Simulink for each quadcopter. The identical initial control values were applied for both quadcopters. The plus-configuration creates a yaw moment when a pitch or roll control input is supplied using multi-rotor controls; however, the cross-configuration decouples pitch and roll control from yaw. However, the plus-quad showed considerable instability while rotating with a pitch and rolling due to the self-generated residual rotation of the four rotors, which is small in the cross quadcopter, making it more maneuverability stable. The obtained results showed that both quadcopters consume the same energy amount.

Keywords: *Quadcopter configuration, PID control, plus configuration, cross configuration, throttle control*

1. INTRODUCTION

The quadrotor, often known as a quadcopter, is a form of unmanned aerial vehicle (UAV) that can take off and land vertically. Because of its intrinsic dynamic nature, the quadrotor has a maneuverability advantage. Mean–while, the small size of such UAVs makes them ideal for specific uses, such as surveillance, military missions, and other fields, such as earth sciences. In UAVs, vision systems could address areas like object identification and tracking. Quadrotors have piqued academics' inte–rest because of their capacity to accomplish tasks quickly and precisely. The focus has now switched to modifying the quadrotor design to overcome its const–raints.

There are two essential quadcopter configurations, as shown in Figure 1, which are the plus and cross con–figurations. Both quadcopter configurations have four rotors attached to the fuselage by arms in a square arra–ngement. The quadcopter has two sets of opposing ro–tors, rotating in opposing directions, as shown in Fig. 1.

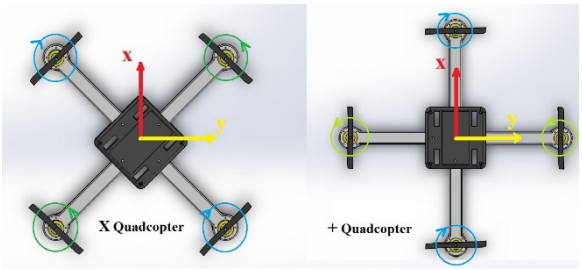

Figure 1. Quadrotor flight configurations

Both forms have attracted many researchers to in–vestigate their configuration on their dynamics. Ahmed H. Ahmed et al. [1]constructed a plus quad–copter mat–hematical model based on MATLAB /Simulink. This study employed a nonlinear mathematical model of the quadcopter, then linearized the model. The transfer fun–ction of the quadcopter's brushless DC motors' attitude controller was obtained using the system identification approach. A detailed test experiment was conducted to determine the designed controller's performance. Gordon Ononiwu et al. [2] described the design and construction of a payload-carrying quadcopter. It was theoretically represented by creating a MATLAB Proportional Integ–ral Derivative (PID) controller. The actual system then used the PID controller settings. The simulation and prototype outputs were compared with and without disturbances. The quadcopter proved to be stable and able to adapt to environmental disturbances.

Ahmed Elrubyet al. [3] focused on a quadrotor mathematical model. A CAD model was constructed to estimate the physical object's mass and inertia. A PID controller for the suggested model is provided, followed by a Simulink model for predicting flight dy–namics response. Zaid Tahir et al. [4] This work develops a linear mathematical model for a quadcopter UAV. They are derived from fundamental Newtonian equations on three degrees of freedom (3DOF) and six degrees of freedom (6DOF) to find state space. The models are critical for controlling the dynamically unstable quad–copter system. Kyaw Myat and Gavrilova [5] described a novel quadcopter design and control technique based on L1 adaptive control, where control parameters are selected systematically by the designer's intended performance and robustness criteria. Asma Katiar et al. [6] used PID and SMC (sliding mode con–trol) control approaches to create a quadcopter dyna–mics controller for hovering maneuvers. Compared to prior research with identical input conditions, the simulation findings reveal an

Received: January 2022 , Accepted: October 2022
Correspondence to: Alaa Abdulhady Jaber, Assistant Professor, Mechanical Engineering Department, University of Technology, Iraq
E-mail: Alaa.A.Jaber@uotechnology.edu.iq
doi: 10.5937/fme2204683M

enhanced response when using the proposed controller. Pengcheng Wang et al. [7] proposed a cascade PID feedback control technique to maintain a cross quad–copter's balancing condition in the face of disturbances. Applying the Newton-Euler technique, the mathematical model of quadcopter dynamics showed precise relationships between all variables. Then, non–linear state-space equations were obtained, which are required for controller design and development. The simulation results showed the cascade PID algorithm's efficacy and resilience compared to the standard PID control strategy. Sevkuthan and Migdat [8] worked on a plus quadcopter control system using LQ and LQG methods. The findings of the continuous and discrete-time altitude and attitude controllers were reported. First, a nonlinear mathematical model for 6 DOF was obtained. Then, the nonlinear model was linearized in hovering mode, and the resultant linear model was reduced to be utilized as a starting model for the controller design. The model was then tested for controllability and observability. The control aim was to track a spatial trajectory with the quad–copter's center of gravity. A Kalman filter state obser–ver was added to the planned LQ controller. The resul–ting controllers accurately regulated the input reference signal and solved the regulatory challenges.

Salma and Osman [9] provided a mathematical model of the DJI F450 UAV quadcopter based on the PID control system for attitude feedback. A rudimen–tary PID is implemented using the DJI F450's parameters for the system. Data of PID control system simulation using DJI F450 quadcopter frame model. The mathematical model for the DJI F450 quadcopter is constructed using Newton-Euler. The simulation is done in MATLAB using the Simulink toolkit. The control system gets altitude data from the Simulink simulation's analysis. This document helps us compre–hend the process of building a quadcopter's entire control system. Other quadcopter mathematical models may be developed quickly utilizing stages with their parameters. Gopalakrishnan Eswar Murthi [10] created a nonlinear model for the plus quadcopter based on motion and moment forces equations. The controller for the nonlinear model was designed, and the results were analyzed. For the given simulation time, the performance of the quadcopter model with the optimal controller values was studied by analyzing the 3-dimensional visualization, the angular velocity, and the angular displacement of the model.

From the previously reviewed papers, it can be noticed that many researchers have worked on various projects and developments for both plus and cross quad–copters. However, they still need to investigate the per–formance differences between the two configurations or why the cross-type quadcopter has become the most popular and widely produced. Thus, in this research, the differences between the two quadcopter configurations will be justified by considering the following:

1-The differences in their mathematical models.

2- The quadcopters' performance and responsiveness to all motion types.

3-The energy consumption by applying the same control system to the two dynamic models.

2. MATHEMATICAL MODELING

This section presents basic concepts and explains the reference frames used in quadcopter flight kinematics. In addition, the logic of quadcopter flight control is specified, and the mathematical model is obtained. The Yaw-Pitch-Roll (YPR) rotation model is widely used, where the angles are around the axis of Z-Y-X, as shown in Figures 2A and 2B for the plus and cross quadcopter configurations. For different factors, com–mon aerospace terms are used.

2.1 KINEMATIC MODEL

Generally, there are four actuators on the quadcopter. Each is composed of a blade, a motor, and a power bridge. Blades 2 and 4 rotate with angular velocities of Ω_2 and Ω_4 in the counter-clockwise direction, while blades 1 and 3 rotate with angular velocities of Ω_1 and Ω_3 in the clockwise direction, as shown in Figure 2(A, B). Notice that the linear movement of the quadcopter as the actuators from 1 to 4 are forward, backward, left and right, and level.

The quadcopter movement's mechanisms can be described as follows:

• Applying equal thrust to all four rotors, the quadcopter hovers or changes its height (up or down).

• Applying high thrust to rotors spinning in one direction changes the angle along with the yaw rotation axis.

• Adding more thrust to one side and less thrust to the diametrically opposite side changes its pitch or roll (x or y movement).

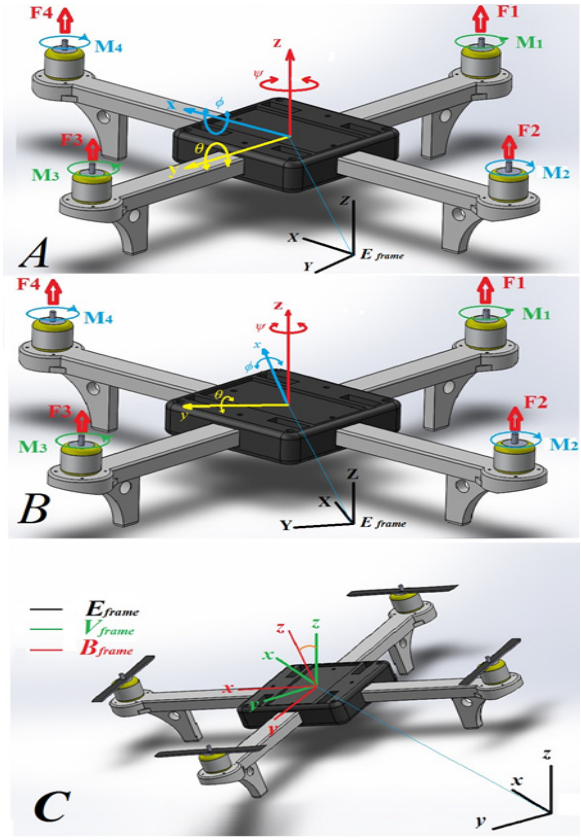

Figure 2. A- Plus quadcopter, B- Cross quadcopter, and C- illustration coordinate frames

Different reference frames and coordination structures are used to define a quadcopter's position and orientation. The transition between them must be carefully considered, such as the Earth and Body frames. The Earth Inertial Frame (E_{frame}) is a fixed Earth coordinate system located at the stated home position. As can be seen in Figure 2, the E_{frame}vectors i (X-axis), j (Y-axis), and k (Z-axis) are directed north, east, and upward from the center of the earth.The Vehicle Inertial Frame (V_{frame}) is located on the quadcopter's center of mass. The axes of V_{frame} are aligned with the axes of E_{frame}. The Fixed Body Frame (B_{frame}) location is also on the quadcopter's center of mass, as the V_{frame}. Initially, it matches with V_{frame}, and its rotation changes to V_{frame} according to the Y-P-R movements. The X-axis points out the nose of the fuselage in every quadcopter location, the Y-axis points out the left side, and the Z-axis points to the top. Based on Figure 2C, the transformation from the V_{frame}tothe $B_{frame}$is described by:

$$M_B = \begin{bmatrix} M_\phi \\ M_\theta \\ M\varphi \end{bmatrix} \tag{1}$$

$$R_v^b(\Phi,\Theta,\Psi) = \begin{bmatrix} 1 & 0 & 0 \\ 0 & \cos\Phi & \sin\Phi \\ 0 & -\sin\Phi & \cos\Phi \end{bmatrix} \begin{bmatrix} \cos\Theta & 0 & -\sin\Theta \\ 0 & 1 & 0 \\ \sin\Theta & 0 & \cos\Theta \end{bmatrix} \begin{bmatrix} \cos\Psi & \sin\Psi & 0 \\ -\sin\Psi & \cos\Psi & 0 \\ 0 & 0 & 1 \end{bmatrix} \tag{2}$$

Rotation from the $B_{frame}$to $V_{frame}$is defined via:

$$R_b^v(\Phi,\Theta,\Psi) = [R_v^b(\Phi,\Theta,\Psi)]^{-1} = [R_v^b(\Phi,\Theta,\Psi)]^T$$
$$R_v^b = \begin{bmatrix} c(\theta)c(\varphi) & s(\varphi)c(\psi)-c(\varphi)s(\psi) & c(\varphi)s(\theta)c(\psi)+s(\varphi)s(\psi) \\ c(\theta)s(\varphi) & s(\varphi)s(\theta)+c(\varphi)s(\psi) & c(\varphi)s(\theta)s(\psi)-s(\varphi)c(\psi) \\ -s(\theta) & s(\varphi)c(\theta) & c(\varphi)c(\theta) \end{bmatrix} \tag{3}$$

where Φ, Θ, Ψ the pitch, roll, and yaw angles, respectively. R_b^v is the rotation matrix from V_{frame} to B_{frame}, s= *sin, c = cos*.

2.2 DYNAMIC MODEL

Quadcopter's dynamics are nonlinear and consist of two multiple subsystems, including full-actuated subsystems that are rotational movements (roll, pitch, and yaw) and Z-axis movement, whereas the under-actuated translational movements in X and Y axes shape the under-actuated movements.

2.3 ROTATIONAL MOTIONS

The rotational movement equations in the body system are derived using the Newton-Euler formulation starting from the following general equation [11].

$$J\dot{W} + W \times JW + M_G = M_B - M_d \tag{4}$$

where J is the quadcopter's inertia matrix in (kg·m^2), $\dot{W}$ is the angular acceleration matrix (rad/sec^2)(pitch, roll, and yaw) in the B_{frame}, W is the angular rates vector (pitch, roll, and yaw) in the B_{frame}(rad/sec), MB is the moments on the quadcopter body frame (N.m), M_G is the gyroscopic moments attributable to rotor activity inertia (N.m), and MD is the drag moment caused by air friction.

$$J = \begin{bmatrix} I_x & 0 & 0 \\ 0 & I_y & 0 \\ 0 & 0 & I_z \end{bmatrix} \tag{5}$$

$$W = \begin{bmatrix} p \\ q \\ r \end{bmatrix} \tag{6}$$

$$\dot{W} = \begin{bmatrix} \dot{p} \\ \dot{q} \\ \dot{r} \end{bmatrix} \tag{7}$$

$$M_B = \begin{bmatrix} M_\phi \\ M_\theta \\ M\varphi \end{bmatrix} \tag{8}$$

I_x, I_y and I_z are the mass moments of inertia in the X, Y, and Z axes, respectively, in the B_{frame} reference.

$$M_G = \begin{bmatrix} 0 \\ 0 \\ J_r\Omega_r \end{bmatrix} \tag{9}$$

where J_r is the rotor's inertia, Ω_c is the residual of rotational velocity, which can be calculated as follows:

$$\Omega_r = -\Omega_1 + \Omega_2 - \Omega_3 + \Omega_4 \tag{10}$$

$\Omega_{1,2,4}$ are the speeds of the four motors.
Ω_r is the problem in the plus quadcopters when they pitch or roll because it is known that the most stable quadcopter has to have zero or very small residual speed. Matrix transformations can be used to locate the components of angular rates and accelerations of the body frame from Euler angles of the earth frame.

$$\begin{bmatrix} p \\ q \\ r \end{bmatrix} = T^{-1} \begin{bmatrix} \dot{\phi} \\ \dot{\theta} \\ \dot{\psi} \end{bmatrix} \tag{11}$$

$$\begin{bmatrix} \dot{p} \\ \dot{q} \\ \dot{r} \end{bmatrix} = T^{-1} \begin{bmatrix} \ddot{\phi} \\ \ddot{\theta} \\ \ddot{\psi} \end{bmatrix} \tag{12}$$

$$T = \begin{bmatrix} 1 & \sin\phi\tan\theta & \cos\phi\tan\theta \\ 0 & \cos\phi & -\sin\phi \\ 0 & \sin\phi & \cos\phi\cos\theta \end{bmatrix} \tag{13}$$

$$T^{-1} = \begin{bmatrix} 1 & 0 & -\sin\theta \\ 0 & \cos\phi & \sin\phi\cos\theta \\ 0 & \sin\phi & \cos\phi\cos\theta \end{bmatrix} \tag{14}$$

Suppose the Euler angles are assumed to be minimal (near 0). In this case, the T^{-1} matrix becomes an identity matrix, and the angular rates are approximately equal to the time derivatives of Euler angles.

2.4 EXTERNAL FORCES, TORQUES, AND AERODYNAMIC EFFECTS

The weight of the quadcopter is a force applied to the quadcopter's center of gravity. It is directed toward the earth's center and written as:

$$F_g = m * g \tag{15}$$

The Propeller Force is the linear force of the pro–pellers, and it is strictly proportional to the speed of the rotors. A single rotor's thrust force is proportional to the square speed of the rotor [add ref.].

$$F_i = K_f \Omega_i^2 \tag{16}$$

where F_i is the thrust force, K_f is the aerodynamic force constant depending on the motor and propeller, can be computed experimentally by measuring rotation speed vs. weight scalar (thrust force) as shown below, then applying Equation 16 to find K_f.

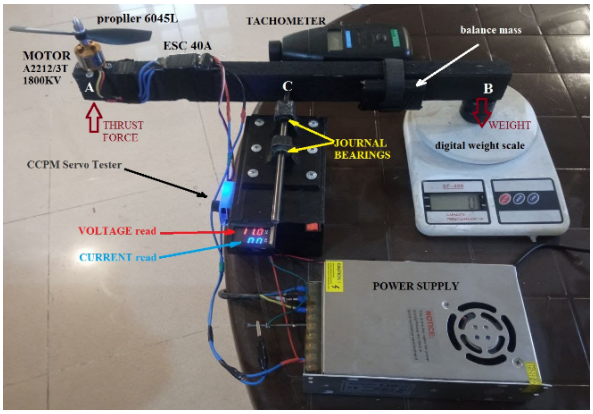

Figure 3. The developed test rig to find the characteristics of the used motor and propeller

The Hub Torque of the propellers is responsible for yaw rotation in the quadcopter; its effect is defined as [12]:

$$M_i = K_h \Omega_i^2 \tag{17}$$

where: i=1, 2, 3, 4. And M_i is the aerodynamic moment, K_h is the aerodynamic moment constant depending on the motor and propeller can be computed experimen–tally by measuring rotation speed versus the generated torque (M_c = weight× arm length) as shown below in Figure 4, then applying Equation 17 to find K_h.

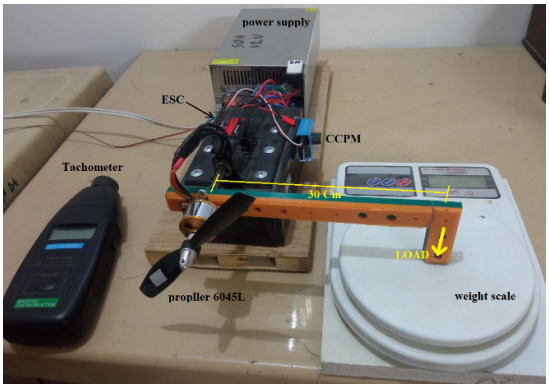

Figure 4. The developed test rig to find the aerodynamic moment constant (K_h)

By evaluating the aerodynamic forces and moments induced by propellers, the three $M_Ø$, M_θ, and M_φ com–ponents of M_B can be obtained. Each propeller generates an upward thrust force F_i and produces a moment M_i with the rotational direction of the corresponding rotor in the opposite direction.

3. CROSS-QUADCOPTER CONFIGURATION

When there is a difference between the summation of F_4 and F_3 and the summation of F_1 and F_2, the rolling moment ($M_Ø$) has to be multiplied by $L/\sqrt{2}$, which is the half dimension between the two forces' action lines. There is a rolling moment ($M_Ø$) about X-axis, as shown in Figure 5.

$$\begin{aligned} M_\phi &= \left(F_4 + F_3 - F_1 - F_2\right) L / \sqrt{2} = \\ &= \left(\Omega_4^2 + \Omega_3^2 - \Omega_1^2 - \Omega_2^2\right) L K_f / \sqrt{2} \end{aligned} \tag{18}$$

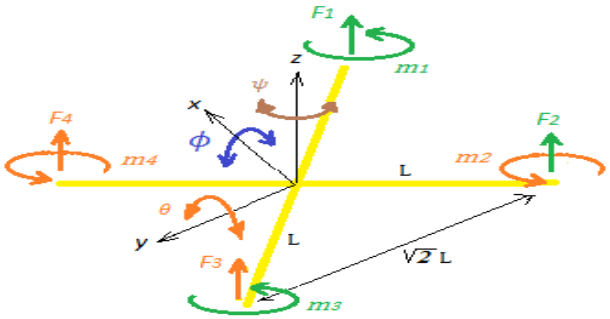

Figure 5. Cross-quadcopter general motions

Similarly, the pitching moment M_θ about the X-axis can be obtained as follow:

$$\begin{aligned} M_\theta &= \left(F_4 + F_3 - F_1 - F_2\right) L / \sqrt{2} = \\ &= \left(\Omega_4^2 + \Omega_3^2 - \Omega_1^2 - \Omega_2^2\right) L K_f / \sqrt{2} \end{aligned} \tag{19}$$

The resultant reactions of the four aerodynamic mo–ments of rotors generate the yawing torque M_φ in the body frame around the Z-axis.

$$\begin{aligned} M_\varphi &= M_1 - M_2 + M_3 - M_4 = \\ &= K_H \left(\Omega_1^2 - \Omega_2^2 + \Omega_3^2 - \Omega_4^2\right) \end{aligned} \tag{20}$$

By substituting Equations 18, 19, 20 in Equation 8, M_B becomes:

$$M_B = \begin{bmatrix} M_\phi \\ M_\theta \\ M_\varphi \end{bmatrix} = \begin{bmatrix} \left(\Omega_4^2 + \Omega_3^2 - \Omega_1^2 - \Omega_2^2\right) L K_f / \sqrt{2} \\ \left(\Omega_3^2 + \Omega_2^2 - \Omega_1^2 - \Omega_4^2\right) L K_f / \sqrt{2} \\ \left(\Omega_1^2 - \Omega_2^2 + \Omega_3^2 - \Omega_4^2\right) K_H \end{bmatrix} \tag{21}$$

The quadcopter has four inputs to four separate rotors, each corresponding to a certain motion form. Hence, the controllable parameter for the quadcopter is the angular velocity of its rotors. Thus, the control inputs vector can be written as $U = [u_1,u_2,u_3,u_4]$ where each input can be obtained as follows:

$$\left.\begin{aligned} u_1 &= \left(\Omega_1^2+\Omega_2^2+\Omega_3^2+\Omega_4^2\right)K_f \ \ throttle\,control \\ u_2 &= \left(\Omega_3^2+\Omega_2^2-\Omega_1^2-\Omega_4^2\right)LK_f \ / \sqrt{2} \ \ roll\,control \\ u_3 &= \left(\Omega_4^2+\Omega_3^2-\Omega_1^2-\Omega_2^2\right)LK_f \ / \sqrt{2}\, pitch\,control \\ u_4 &= \left(\Omega_1^2-\Omega_2^2+\Omega_3^2-\Omega_4^2\right)K_H \ \ yaw\,control \end{aligned}\right\} \quad (22)$$

Equation 23 below is called the motor mix algorithm [13], which converts the control input vector (u_1,u_2, u_3,u_c) to motors speeds (Ω1,Ω2,Ω3,Ω4).

$$\begin{bmatrix}\Omega_1^2\\ \Omega_2^2\\ \Omega_3^2\\ \Omega_4^2\end{bmatrix} = \frac{1}{4}\begin{bmatrix} 1/K_f & -\sqrt{2}/LK_f & -\sqrt{2}/LK_f & 1/K_H \\ 1/K_f & -\sqrt{2}/LK_f & \sqrt{2}/LK_f & -1/K_H \\ 1/K_f & \sqrt{2}/LK_f & \sqrt{2}/LK_f & 1/K_H \\ 1/K_f & \sqrt{2}/LK_f & -\sqrt{2}/LK_f & -1/K_H \end{bmatrix}\begin{bmatrix}u_1\\ u_2\\ u_3\\ u_4\end{bmatrix} \quad (23)$$

Plus-Quadcopter Configuration

When there is a disparity in the values of the forces F_4, with F_2 and F_3 with F_1multiply by L, which is the half dimension between the two forces results in an action line, there was the rolling moment M_c about X-axis, as $\begin{bmatrix}\Omega_1^2\\ \Omega_2^2\\ \Omega_3^2\\ \Omega_4^2\end{bmatrix}$ shown in Figure 5.

$$M_\phi = \left(F_4 - F_2\right)L = \left(\Omega_4^2 - \Omega_2^2\right)LK_f \quad (24)$$

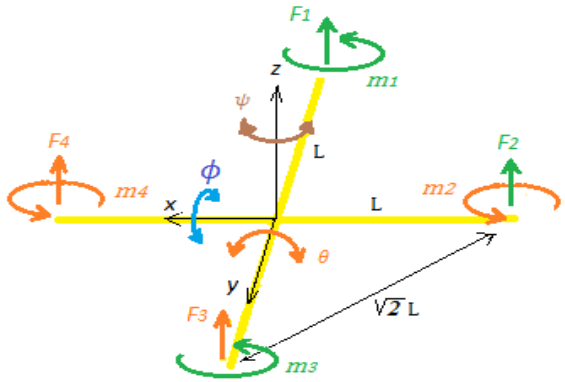

Figure 6. Plus-quadcopter general motions

Following the same way as in the cross-quadcopter, the pi–tching moment about Y-axis can be obtained as follows:

$$M_\theta = \left(F_3 - F_1\right)L = \left(\Omega_3^2 - \Omega_1^2\right)LK_f \quad (25)$$

The resultant reactions of the four aerodynamic moments of rotors generate the yawing torque (M_φ) in the body frame around the Z-axis.

$$M_\varphi = M_1 - M_2 + M_3 - M_4 = K_H\left(\Omega_1^2 - \Omega_2^2 + \Omega_3^2 - \Omega_4^2\right) \quad (26)$$

By substituting Equations 24,25,26 in Equation 8, M_B becomes:

$$M_B = \begin{bmatrix}M_\phi\\ M_\theta\\ M_\varphi\end{bmatrix} = \begin{bmatrix}\left(\Omega_4^2-\Omega_2^2\right)LK_f\\ \left(\Omega_3^2-\Omega_1^2\right)LK_f\\ K_H\left(\Omega_1^2-\Omega_2^2+\Omega_3^2-\Omega_4^2\right)\end{bmatrix} \quad (27)$$

Hence, the control inputs vector, which contains four controllable parameters, is U = [u_1,u_2,u_3,u_4] where each input:

$$\left.\begin{aligned} u_1 &= K_f\left(\Omega_1^2+\Omega_2^2+\Omega_3^2+\Omega_4^2\right) \ altitude \\ u_2 &= LK_f\left(\Omega_4^2-\Omega_2^2\right) \ roll\,attitude \\ u_3 &= LK_f\left(\Omega_1^2-\Omega_3^2\right) \ pitch\,attitude \\ u_4 &= K_H\left(\Omega_1^2-\Omega_2^2+\Omega_3^2-\Omega_4^2\right) \ yaw\,attitude \end{aligned}\right\} \quad (28)$$

$$\begin{bmatrix}u_1\\ u_2\\ u_3\\ u_4\end{bmatrix} = \begin{bmatrix} k_f & k_f & k_f & k_f \\ 0 & -Lk_f & 0 & LK_f \\ LK_f & 0 & -LK_f & 0 \\ k_H & -k_H & k_H & -k_H \end{bmatrix}\begin{bmatrix}\Omega_1^2\\ \Omega_2^2\\ \Omega_3^2\\ \Omega_4^2\end{bmatrix} \quad (29)$$

$$\begin{bmatrix}\Omega_1^2\\ \Omega_1^2\\ \Omega_3^2\\ \Omega_4^2\end{bmatrix} = \frac{1}{4}\begin{bmatrix} 1/k_f & 0 & 1/Lk_f & 1/k_H \\ 0 & -1/Lk_f & 0 & -1/k_H \\ 1/k_f & 0 & -1/Lk_f & 1/k_H \\ 1/k_f & 1/Lk_f & 0 & -k_H \end{bmatrix}\begin{bmatrix}u_1\\ u_2\\ u_3\\ u_4\end{bmatrix} \quad (30)$$

Translational motions

Newton's second law [11] can be used to define the translational motion of a body:

$$F_d = K_d\dot{r}^2 \quad (31)$$

F is the difference value between thrust force and gravity, where $\ddot{r}$ is the acceleration of the quadcopter from the earth frame and equals to:

$$\ddot{r} = \begin{bmatrix}\ddot{r}_x\\ \ddot{r}_y\\ \ddot{r}_z\end{bmatrix} \quad (32)$$

The total thrust that rotors produce is only one com–ponent in the Z-direction, and it is calculated by:

$$F_{th} = F_1 + F_2 + F_3 + F_4 \quad (33)$$

Substituting Equation 7 in the above equation gives:

$$F_{th} = K_f\left(\Omega_1^2+\Omega_2^2+\Omega_3^2+\Omega_4^2\right) \quad (34)$$

The only non-gravitational force remaining in action is when the quadcopter is in a steady-state condition. Equation 13 will be [14,15]:

$$m\begin{bmatrix}\ddot{r}_x\\ \ddot{r}_y\\ \ddot{r}_z\end{bmatrix} = \begin{bmatrix}0\\ 0\\ -mg\end{bmatrix} + R_v^b\begin{bmatrix}0\\ 0\\ F_{th}\end{bmatrix} - F_d \quad (35)$$

The rotation matrix R_v^b should be multiplied by F_{th}. In order to obtain the thrust forces of the rotors in the

earth frame. In this way, the equation is valid for every orientation of the UAV quadcopter. As shown in Equation 23, the zero values in the force vector imply that there is no force in the X and Y directions, while the third row in the matrix is simply an extension of the thrust forces supplied by the four propellers. Aerodynamic effects [16] are added to the equation by considering the drag forces (F_d), which can be accessed through:

$$F_d = K_d \dot{r}^2 \tag{36}$$

where $\dot{r}$ is the time derivative of the position vector, which equals to $\left[\dot{r}_x, \dot{r}_y, \dot{r}_z\right]^T$ and K_d is the drag force constant, which depends on the outside area of the quadcopter and air density as follows[17]:

$$K_d = \frac{1}{2}\rho C_D A \tag{37}$$

where ρ is the air density (kg⁄m^3), C_D is the aerodynamic drag coefficient, and A is the effective area (m^2).
K_d for both plus and cross quadcopter was calculated directly using the SolidWorks Flow Simulator. Drag force constants in the Z direction are the same for each configuration because they have the same effective area, but in the X or Y directions, the constants have different values because the different effective areascause different isosurfaces (airflow distribution in the space) and flow trajectories at the same X speed motion, as shown in Figure 7.

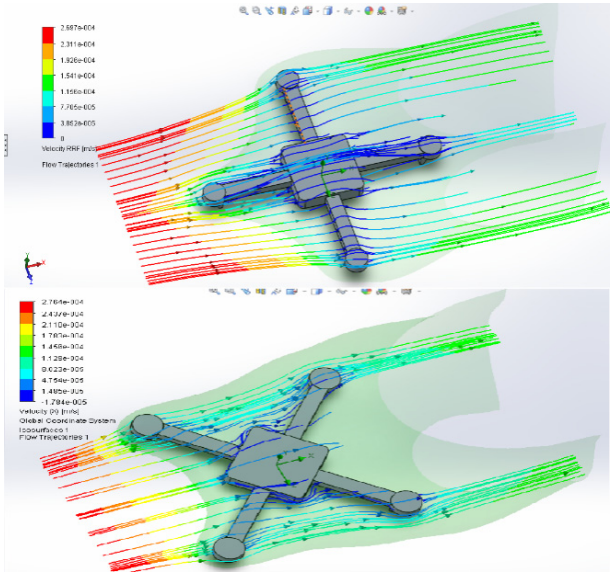

Figure 7. plus and cross quadcopter flow trajectories

Going back to Equation 2 and substituting each term with its corresponding will get:

$$\begin{bmatrix} I_x & 0 & 0 \\ 0 & I_y & 0 \\ 0 & 0 & I_z \end{bmatrix} \begin{bmatrix} \ddot{\phi} \\ \ddot{\theta} \\ \ddot{\psi} \end{bmatrix} + \begin{bmatrix} p \\ q \\ r \end{bmatrix} \times \begin{bmatrix} I_x & 0 & 0 \\ 0 & I_y & 0 \\ 0 & 0 & I_z \end{bmatrix} \times \begin{bmatrix} p \\ q \\ r \end{bmatrix} + \begin{bmatrix} p \\ q \\ r \end{bmatrix} \times \begin{bmatrix} 0 \\ 0 \\ J_r\Omega \end{bmatrix} = \begin{bmatrix} lu_2 \\ lu_3 \\ u_1 \end{bmatrix} \tag{38}$$

Hence, the angular accelerations of the quadcopter can be presented as follows:

$$\ddot{\phi} = \dot{\psi}\dot{\theta}\left(\frac{I_y - I_z}{I_x}\right) - \frac{J_r}{I_x}\dot{\theta}\Omega_r + \frac{l}{I_x}u_2 \tag{39}$$

$$\ddot{\theta} = \dot{\psi}\dot{\phi}\left(\frac{I_y - I_x}{I_z}\right) + \frac{J_r}{I_x}\dot{\theta}\Omega_r + \frac{l}{I_y}u_3 \tag{40}$$

$$\ddot{\psi} = \dot{\phi}\dot{\theta}\left(\frac{I_y - I_z}{I_x}\right) + \frac{l}{I_z}u_4 \tag{41}$$

Applied and represent the equation of translation motion (23) to find ($\ddot{x}, \ddot{y}, \ddot{z}$) parameters. Substitute each term with its corresponding equation. Will get:

$$m\begin{bmatrix} \ddot{x} \\ \ddot{y} \\ \ddot{z} \end{bmatrix} = \begin{bmatrix} 0 \\ 0 \\ -mg \end{bmatrix} + R_b^v \begin{bmatrix} 0 \\ 0 \\ u_1 \end{bmatrix} - K_d \begin{bmatrix} \dot{x} \\ \dot{y} \\ \dot{z} \end{bmatrix} \tag{42}$$

$$m\begin{bmatrix} \ddot{x} \\ \ddot{y} \\ \ddot{z} \end{bmatrix} = \begin{bmatrix} 0 \\ 0 \\ -mg \end{bmatrix} + \begin{bmatrix} (S\phi S\psi + C\phi S\theta C\psi)u_1 \\ (S\phi S\psi - C\phi S\theta C\psi)u_1 \\ (C\phi C\theta)u_1 \end{bmatrix} - K_d \begin{bmatrix} \dot{x} \\ \dot{y} \\ \dot{z} \end{bmatrix} \tag{43}$$

$$\ddot{x} = \frac{u_1}{m}(S\phi S\psi + C\phi S\theta C\psi) - \frac{K_{dx}}{m}\dot{x} \tag{44}$$

$$\ddot{y} = \frac{u_1}{m}(C\phi S\psi S\theta + S\phi C\psi) - \frac{K_{dy}}{m}\dot{y} \tag{45}$$

$$\ddot{y} = \frac{u_1}{m}(C\phi S\psi S\theta + S\phi C\psi) - \frac{K_{dy}}{m}\dot{y} \tag{46}$$

As a result, adjusting the roll and pitch angles allows effect movement along the X and Y axes.

PID Control system

PID stands for Proportional, Integral, and Derivative, and it is a feature of flight controller software that analyzes sensor data and determines how quickly the motors should spin to keep the quadcopter rotating at the appropriate speed, Figures 8 and 9. The PID controller's objective is to reduce "error", which is the difference between a measured value (gyro sensor measurement)[18] and the desired set-point (the desired rotation speed). The proportional component of the PID preserves quadcopter stability, while the integral component accomplishes precision and the derivative component controls speed. The relevant gains (P, I, and D) must be fine-tuned for better control performance [19]. Hence, the tuning method offered by MATLAB Simulink was utilized for this purpose [19]. The MATLAB optimization tool makes adjustments to the inputs in order to produce the appropriate output signal based on the conditions that have been predefined. A series of simulations was carried out until the best feasible combination of parameters was discovered to produce output signals that were identical to the input signals. In the Simulink software, the same continuous-time PID controller was used for each quadcopter configuration, the reason is that there is no difference in the dynamic models and equations of motion, but only the difference between them lies in the mix of speeds logarithms (23

and 30), which can be found from the PID outputs so that PID will be the same in both configurations.

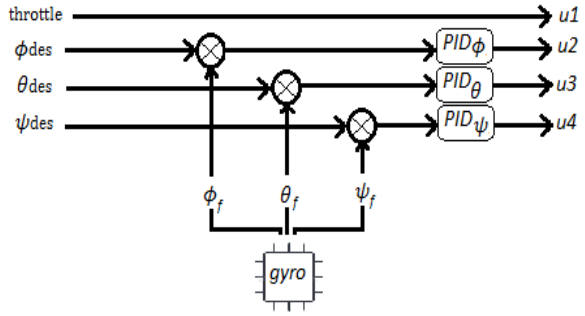

Figure 8. PID control systems

Frame parameters

The total weight of the quadcopter once the electrical components were attached was 841 grams, considering the mass distribution and densities for each component and the magnitude of the mass moment of inertia for the two quad–copters around each axis calculated based on SolidWorks software [20], as shown in Table (2). The other parameters, such as K_h, and K_f, were found experimentally.

Table 1. Quadcopter parameters

Parameter	Value
m	0.841 Kg
L	30 Cm
K_H	$1.3858*10^{-6}$ N.m.s^2
K_f	$1.3328*10^{-5}$ N.s^2
Jr	0.0045 kg.m^2
Cross quad Kd_x,Kd_y	0.1040 kg/m
plus quad Kd_x,Kd_y	0.1465 kg/m
kd_z	0.4044 kg/m

Table 2. Mass moment of inertia

	I_x	I_y	I_z
Cross Quadcopter	0.01121	0.01114	0.02179
Plus Quadcopter	0.01105	0.01111	0.02179

Table 3. The obtained PID gains

	K_P	K_I	K_D
Roll	0.2082	0.01214	0.7931
Pitch	0.2082	0.01214	0.7931
Yaw	0.0507	0.00296	0.1933

Methodology

The control systems for both plus and cross quadcopter configurations are connected to the same set-point inputs. First, they were given a rolling angle of 45^0, and the six signals (the pitch, roll, and yaw from each quadcopter), the set-point, and feedback were collected in one scope to be easily investigated. The process was then repeated for each pitch, yaw, and quad separately. The Simulink in Figure 9 shows in the (motor mix algorithm block) the difference between the cross and plus quadcopter as motor mix algorithm equations (10, 23, and 30).

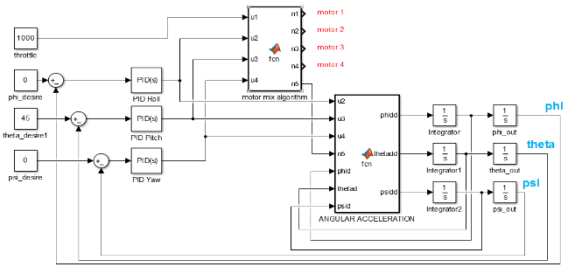

Figure 9. Simulink PID quadcopter system

Power consumption

UAVs are typically electric vehicles powered by on–board batteries that have a finite lifespan. The short battery life of UAVs has been noted as a significant issue. Hence, in this paper, the effect of quadcopter configuration on the consumed power has been invest–tigated. There are many ways to calculate the consumed power of brushless motors. It can be practically calcu–lated by knowing the instantaneous current taken from the battery and multiplying it by the battery voltage[12], or the total power consumed by each motor is directly proportional to the Hub torque of the rotor part with the propeller (Equation 17) multiplied by the rotation speed (rad/sec).

$$P = M_i \times \Omega_i \tag{47}$$

By summing the energy consumed by all the motors, the total energy consumed for each quadcopter can be estimated. Figure 10 shows the Simulink used for calcu–lating and comparing the consumed power.

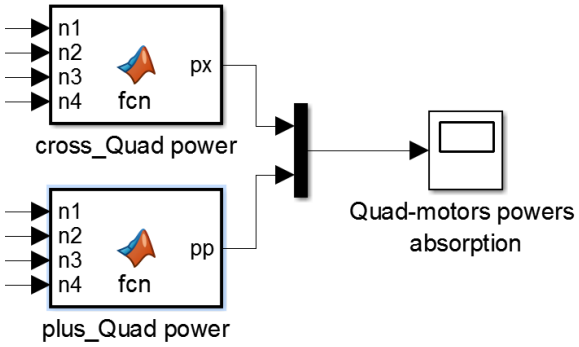

Figure 10. The designedSimulink calculates and compares the energy consumed for each quadcopter

4. RESULTS

The work presented shows that when examining the movement of the two quadcopters in the Z-direction at a certain speed, each of the two quadcopters will show the same resistance to the air when rising or vertical descent because the air-repelling area of the frame from above and below is the same area for the two quadcopters, so the air resistance force for them is equal. However, when moving in the X or Y direction, there is no dif–ference on the same quadcopter because of the sym–metry of the frame. But the difference is between each of the two frames due to the difference in the area and angle of air repelling (see Figure 7). The air trajectories flow is different, which means that the F_d for the cross frame does not equal its value for the plus frame (when

X or Y speed is constant). This is because the effective area of air repelling when traveling in the X or Y direction of the cross quadcopter was 0.0091 m^2, which is less in comparison to the plus quadcopter (0.01356 m^2), and the larger effective area caused confusion and instability as a result of the air impedance of the larger area. So the cross quadcopter's drag force constant (Kd) will be less for the plus quadcopter when traveling in both X and Y directions (see Table 1).

The following figures show the results of applying the identical PID control to both quadcopters. The motors mix algorithm can differentiate between the two quad–copters. For example, to turn the plus-quadcopter to the right (rolling), the speed of motor #3 is increased while the speed of motor #1 is decreased (Figure 2A), and vice versa if it is turned to the left. The same concept can be applied to forward and backward move–ment (pitching). Rotating the quadcopter around itself (yawing) is produced by increasing the speeds of motors #4 and #2 and reducing the speeds of motors #1 and #3 or vice versa. Figure 2B shows the cross quadcopter; if we want the quadcopter to roll to the right, we will raise the speeds of motors#3 and #4 while decreasing the speeds of motors#1 and #2 and vice versa. The same idea applies to forward and backward movement (pitching). The (yawing) is the same as in the plus quadcopter.

As a result of these movements, when Equation 10 is applied to each quadcopter, the difference in the speeds is formed, producing what is previously defined as the residual rotational velocity (Ω_r). As discussed earlier, this speed becomes an issue if its value is significant. For example, Figures 10 and 11 of the plus quadcopter show this when it is pitching. As shown in the above mentioned figures, a minor unstable signal is formed. The pitch transient signal is created when moving with the roll and vice versa. This signal is caused by the formation of Ω_r, which is bigger in the plus quadcopter than in the cross one, as shown in Figures 12 and 13, for the same frame, constants, and control system. As a result, it can be stated that the cross quadcopter is more stable in terms of motions and maneuvering than the plus quadcopter.

Regardless of the pitch, roll, and yaw trim settings, the necessary power at all speeds is the same, as illustrated in Figures 14-16. Also, Figure 17 shows that when quads over are stable, the power of the collective speed is equal to 180 Watts for the two types.

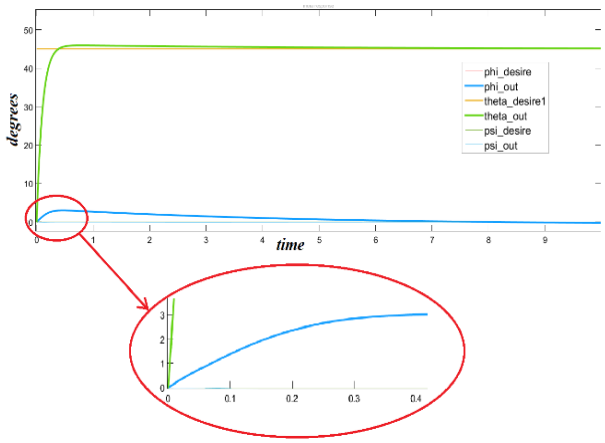

Figure 11. Plus quadcopter pitching response

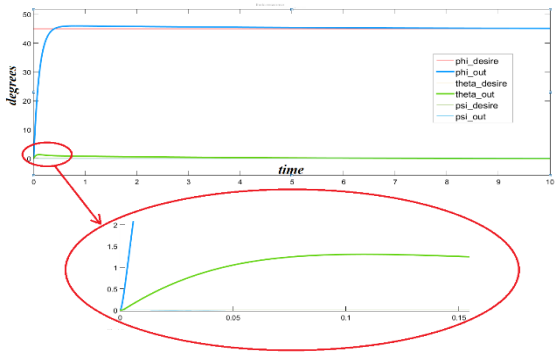

Figure 12.Plus-quadcopter rolling response

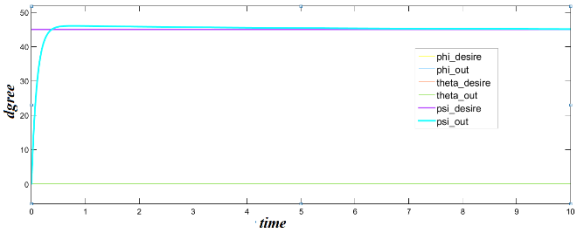

Figure 13. Plus-quadcopter yawing response

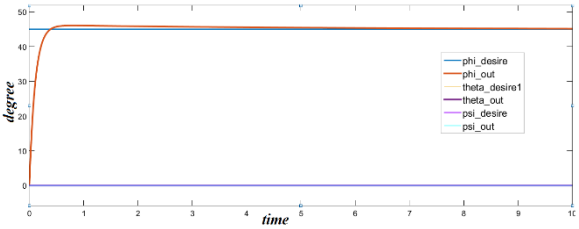

Figure 14. Cross-quadcopter pitching response

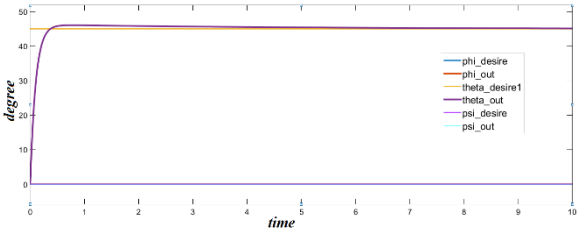

Figure 15. Cross-quadcopter rolling response

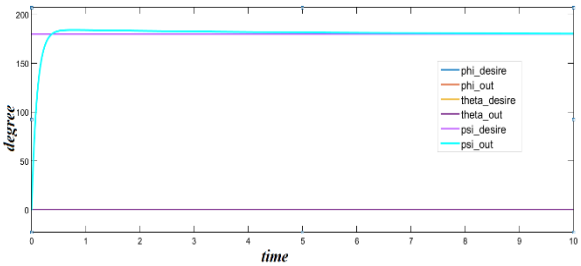

Figure 16. Cross-quadcopter yawing response

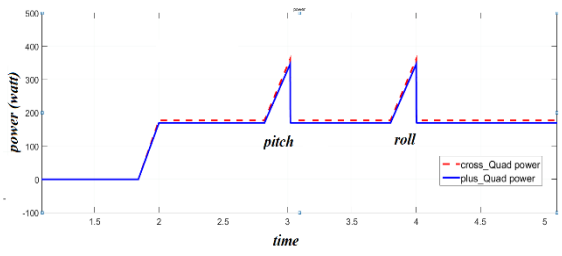

Figure 17.The predicted power consumption for the cross and quadcopters

5. CONCLUSION

The same frames may be utilized in the form of the cross quadcopter and the shape of the plus, according to the previous models and results, and this can be done in two steps:

1- In the plus quadcopter, the body frame axes (X and Y) are parallel to the arms, while in the configuration cross, they are at a 45-degree angle.

2 - The Plus quadcopter has a particular algorithm for controlling the motors based on the motions, and the cross quadcopter has its own algorithm.

In terms of performance, If we take the same frame and make it once in the form cross and once in the form of a plus, the cross quadcopter has been proven to be more stable in maneuvering due to the absence of residual rotational velocity. The aerodynamic analysis of the two frames showed that the drag force when rising up and down for both frames is equal. But it in both directions (pure X or Y) for the plus shape is greater than the cross frame, which causes aerobic swing. In terms of energy consumption, as a theoretical ideal, both quadcopters consume the same amount of energy during all types of movement. However, the plus quadcopter is exposed to a greater drag force than the cross quadcopter, which requires more energy to overcome it. This is the reason behind the cross quadcopter's supremacy and popularity over the plus one and the latter's demise from interest.

REFERENCES

[1] H. Ahmed, Ahmed Kamel, A. N. Ouda and Yehia Z. Elhalwagy, "Design and Analysis of Quadcopter Classical Controller," in *16th International Confe–rence on AEROSPACE SCIENCES & AVIATION TECHNOLOGY*, Kobry Elkobbah, Cairo, Egypt, 2015.

[2] G. Ononiwu, Ondoma Onojo, Oliver Ozioko and Onyebuchi Nosiri, "Quadcopter Design for Payload Delivery," *Journal of Computer and Communi–cations,* vol. 4, no. 10, 2016.

[3] A. Elruby, Mohamed Elkhatib and Noha Hany El-Amary, "Dynamics Modeling and Control of Quadrotor Vehicle," in *Conference: the 5th International conference on Applied Mechanics and Mechanical Engineering*, Cairo, Egyp, 2012

[4] Z. Tahir, Mohsin Jamil, Saad Ali Liaqat and Syed Omer Gilani, "State Space System Modelling of a Quad Copter UAV," *Indian Journal of Science and Technology,* vol. 9, no. 27, July 2016

[5] K. M. Thua and A.I. Gavrilov, "Designing and modeling of quadcopter control system using L1 adaptive control," *Procedia Computer Science,* vol. 103, p. 528 – 535, 2017

[6] A. Katiar, Rabbia Rashdi, Zeeshan Ali and Urooj Baig, "Control and stability analysis of quadcopter," in *International Conference on Computing, Mathematics and Engineering Technologies*, Jamshoro, Pakistan, 2018

[7] Z. M. Z. C. Z. Pengcheng Wang, "Dynamics Modelling and Linear Control," in *International Conference on Advanced Mechatronic Systems*, Melbourne, Australia, 2016

[8] M. H. Sevkuthan KURAK, "Control and Estimation of a Quadcopter Dynamical Model," *Periodicals of Engineering and Natural Sciences,* vol. 6, no. 1, p. 63−75, 2018

[9] N. M. Salma and Khairuddin Osman, "Modelling and PID control system integration for quadcopter DJIF450 attitude stabilization," *Indonesian Journal of Electrical Engineering and Computer Scienc,* vol. 19, no. 3, pp. 1235-1244, 2020

[10] G. E. Murthi, Quadcopter flight mechanics model and control algorithms, Prague, Czech : Czech Technical University, 2016

[11] JL.Meriam and L.G Kraige, "Introduction to three-dimensional dynamic of rigid bodies," in *DYNAMICS*, sixth ed., Virginia, 2010, pp. 527-600

[12] A. R. Firdaus, Design of sliding mode-based nonlinear control systems with nonlinear full-order state observers for underactuated coupled systems, Sheffield,United Kingdom: University of Sheffield, 2018

[13] A. Hussein, Autopilot Design for a Quadcopter, Khartoum: University Of Khartoum, 2017

[14] M. C. D. Simone and D. Guida , "Control Design for an Under-Actuated UAV Model," *FME Transactions ,* vol. 46, no. 4, pp. 443-452, 2018

[15] A. Nemes and Gyula Mester , "Unconstrained Evolutionary and Gradient Descent-Based Tuning of Fuzzy-partitions for UAV Dynamic Modeling," *FME Transactions ,* vol. 45, no. 1, pp. 1-8, (2017)

[16] M. S. Selig, "Modeling Propeller Aerodynamics and Slipstream Effects on Small UAVs in Real–time," in *Atmospheric Flight Mechanics Confe–rence*, Toronto, Ontario, Canada, 2010

[17] M. C. D. Simone and D. Guida, "Control Design for an Under-Actuated UAV Model," *FME Transactions,* vol. 46, pp. 443-452, 2018

[18] B. Sumantri, ni'am tamami, Yudha Birawa Nuraga and Bagus Kurniawan, "Development of a Low-Cost Embedded Flight Controller for Quadcopter," *International Electronics Symposium (IES),* pp. 233-238, 2020

[19] M. Ristanović, Dragan Lazić and Ivica Inđin, "Experimental Validation of Improved Performances of an Electromechanical Aerofin Control System With a PWM Controlled DC Motor," *FME Transactions ,* vol. 34, no. 1, pp. 15-20, 2006

[20] S. Team, "Mass Moments of Inertia," SolidWORKS, 2022. [Online]. Available: https://help.solidworks.com/2017/english/SolidWorks/motionstudies/HIDD_BLOCK_INERTIA.htm

NOMENCLATURE

$Ø$	roll angle
Θ	pitch angle
Ψ	yaw angle
Ω_i	motor rotation speed
Ω_r	residual rotational velocity
F_i	thrust force
F_d	drag force

G	ground acceleration
I	mass moment of inertia
Jr	rotor inertia
K_f	aerodynamic force constant
K_H	aerodynamic moment constant
L	length of arm
m	mass of quadcopter
M	torque
P	power
u_i	controlinput

ПОРЕЂЕЊЕ ДИНАМИЧКОГ МОДЕЛА И КОНТРОЛЕ ЛЕТА ПЛУС И УНАКРСНИХ КВАДКОПТЕР КОНФИГУРАЦИЈА

К.К. Али, А.А. Цабер

Ово истраживање истражује и показује фунда–менталне разлике у перформансама и раду и унак–рсних и квадкоптерских конфигурација. Нелинеарни динамички модел система је прво изведен и импле–ментиран у Симулинк-у за сваки квадрокоптер. За оба квадрокоптера примењене су идентичне почетне контролне вредности. Плус-конфигурација ствара момент скретања када се улаз за контролу нагиба или превртања напаја помоћу контрола са више ротора; међутим, унакрсна конфигурација раздваја контролу нагиба и превртања од скретања. Међутим, плус-квад је показао значајну неста–билност док се ротирао са кораком и котрљањем због самогенерисане преостале ротације четири ротора, која је мала у унакрсном квадрокоптеру, што га чини стабилнијим у погледу маневрисања. Доби–јени резултати су показали да оба квадрокоптера троше исту количину енергије.